

15-4-1999

Dielectric function of an electron gas under intense laser radiation in quantizing magnetic fields

W. Xu

University of Wollongong

Follow this and additional works at: <https://ro.uow.edu.au/engpapers>



Part of the [Engineering Commons](#)

<https://ro.uow.edu.au/engpapers/243>

Recommended Citation

Xu, W.: Dielectric function of an electron gas under intense laser radiation in quantizing magnetic fields 1999.

<https://ro.uow.edu.au/engpapers/243>

Dielectric function of an electron gas under intense laser radiation in quantizing magnetic fields

W. Xu*

Department of Engineering Physics, Institute for Superconducting & Electronic Materials, University of Wollongong, NSW 2522, Australia

(Received 26 January 1998; revised manuscript received 3 August 1998)

A detailed theoretical study on dielectric function of a three-dimensional electron gas (3DEG), subject to linearly polarized intense laser field and to strong static magnetic field, is presented. Using the Green's-function approach, I have derived the density-density correlation function and the random-phase-approximation dielectric function for a 3DEG in t and Ω representation. It is found that in the presence of intense terahertz laser field, the dielectric function of an electron gas depends strongly on frequency and intensity of the electromagnetic radiation. A number of important radiation effects, pertinent to the application of the free-electron laser sources developed recently, are presented and discussed. [S0163-1829(99)10511-3]

I. INTRODUCTION

The investigation of dielectric function (or dielectric response function) of an electron gas has played an important role in modern condensed-matter physics and electronics. The dielectric function measures the strength of a gas of electrons interacting via their long-range force such as Coulomb potential. Therefore, it is of paramount importance in discussing many-body problem of an electron gas and in studying elementary electronic excitations from an electron gas. In the absence of the *intense* electromagnetic (EM) radiation, the dynamic and static dielectric function of three-dimensional and low-dimensional electron gases (3DEG's and LDEG's) in zero and quantizing magnetic fields has been extensively studied in the past, and the results have been well documented.¹⁻⁴

In recent years, there has been a rapid expansion in developing high-power, long wavelength, and tunable laser sources such as free-electron lasers (FEL's). The current generation of the FEL's has already been able to provide the source of the linearly polarized tunable laser radiations in far-infrared or terahertz (10^{12} Hz or THz) bandwidth.⁵⁻¹⁰ Very recently, the THz FEL radiation has been applied to experimental measurements in investigating nonlinear transport and optical properties in the electron gas devices such as semiconductor systems. Some important and interesting THz radiation phenomena, such as resonant absorption of the THz radiation,⁵ THz photon-enhanced hot-electron effect,⁶ THz photon-induced impact ionization,⁷ LO-phonon bottleneck effect,⁸ THz photon-assisted resonant tunneling,⁹ THz cyclotron resonance,¹⁰ etc., were observed in different semiconductor structures. More importantly, the combination of the THz FEL radiation with static high-magnetic field has been successfully applied to the measurement of magnetotransport properties in semiconductor systems.¹¹ In conjunction with these experimental research activities, it is of value to examine theoretically how an intense laser-field affects such a fundamental quantity like dielectric function of the electron gas in the presence of the quantizing magnetic field, and this is the main motivation of the present study.

From a theoretical point of view, the investigation of an

electron gas under intense laser radiation offers us a possibility to examine and to develop tractable method in handling time-dependent quantum problem. Very recently, I have studied the influence of the intense THz EM radiation on density of states (DoS) for free electrons in one-dimensional¹² and two-dimensional¹³ electron gases and in three-dimensional electron gases in strong magnetic fields.¹⁴ Since the dielectric response of an electron gas is connected directly to the electron DoS or Green's function, one expects that in the presence of the intense THz laser radiation the dielectric function of an electron gas will differ significantly from those observed in the absence of the EM field. In this paper, I perform a detailed theoretical study of the dielectric function of a THz-driven 3DEG in quantizing magnetic fields. In Sec. II, I recall briefly some of the relevant results obtained in Ref. 14. Then, I will derive the electron density-density correlation function (see Sec. III) and the dynamical dielectric function (see Sec. IV) in t and Ω representation, by employing the approaches in dealing with time-dependent problem. The further results for the influence of the intense THz laser radiation on dielectric function of a 3DEG in strong magnetic fields are presented and discussed in Sec. V, and the main conclusions drawn from this study are summarized in Sec. VI.

II. GREEN'S FUNCTION

In this paper, I consider the situation where a static magnetic field B is applied along the z axis of a 3DEG and an EM field $A(t)$ is linearly polarized parallel to B {i.e., $A(t)=[0,0,A_0 \sin(\omega t)]$ with ω being the frequency of the EM field}. In this configuration, the radiation field will not couple *directly* to the magnetic field. As a result, the Landau-level (LL) energy depends very little on applied EM field and the *direct* cyclotron resonance effect is absent. The time-dependent Schrödinger equation for a free electron in this geometry can be solved analytically and the retarded (+) and advanced (-) Green's functions for electron in t space (i.e., time space) are obtained as¹⁴

$$G^+(N, k_z; t > t') = -\frac{i}{\hbar} \Theta(t-t') R(N, k_z; t, t'), \quad (1a)$$

and

$$G^-(N, k_z; t > t') = \frac{i}{\hbar} \Theta(t-t') R(N, k_z; t', t). \quad (1b)$$

Here, $\Theta(x)$ is the unit-step function, N is the index for the N th LL, k_z is the electron wave vector along the z direction, and

$$\begin{aligned} R(N, k_z; t, t') &= e^{-i[E_N(k_z) + E_{em}](t-t')/\hbar} \\ &\times e^{-ir_0 k_z [\cos(\omega t) - \cos(\omega t')]} \\ &\times e^{i\gamma [\sin(2\omega t) - \sin(2\omega t')].} \end{aligned} \quad (1c)$$

In Eq. (1c), $E_N(k_z) = \hbar^2 k_z^2 / 2m^* + E_N$, m^* is the effective-electron mass, $E_N = (N + 1/2)\hbar\omega_c$ is the N th LL energy, $\omega_c = eB/m^*$ is the cyclotron frequency, $r_0 = eF_0/m^*\omega^2$ with $F_0 = A_0\omega$ being the strength of the radiation electric field, $E_{em} = 2\gamma\hbar\omega$ is the energy of the radiation field, and $\gamma = (eF_0)^2 / (8m^*\hbar\omega^3)$.

The Fourier transform of the retarded Green's function and the steady-state electron density of states have been documented and discussed in Ref. 14.

III. ELECTRON DENSITY-DENSITY CORRELATION FUNCTION

In the study of the dielectric response and the many-body properties of an electron gas, the electron density-density ($d-d$) correlation function (or so-called pair bubble) plays an important role. In the presence of a strong magnetic field, the electron $d-d$ correlation function can be derived from the Green's function¹⁵ or from the approach of the density-fluctuation.¹⁶ Since the retarded and advanced Green's functions for a 3DEG subjected to EM and magnetic fields has been obtained, it is straightforward to employ the Green's function approach to the evaluation of the electron $d-d$ correlation function. In the absence of the electron-electron ($e-e$) interaction, the pair bubble in the (\mathbf{Q}, t) -representation is defined by [see Fig. 1(a)]

$$\begin{aligned} -i\Pi(\mathbf{Q}; t, t') &= -i \frac{g_s}{2\pi l^2} \sum_{N', N} D_{N', N}(q) \sum_{k_z} \frac{1}{\beta} \sum_{n=-\infty}^{\infty} \\ &\times [iG^-(N, k_z; t > t') e^{-i\omega_n(t-t')}] \\ &\times [iG^+(N', k_z + q_z; t > t') e^{i\omega_n(t-t')}. \end{aligned} \quad (2)$$

Here, $\beta = 1/k_B T$, $\omega_n = (2n + 1)\pi/\beta$, $\mathbf{Q} = (\mathbf{q}, q_z) = (q_x, q_y, q_z)$, $g_s = 2$ accounts for the spin degeneracy, $l = (\hbar/eB)^{1/2}$, and $1/2\pi l^2$ is the degeneracy of each LL in unit area. Further, $D_{N', N}(q) = C_{N', N}(l^2 q^2/2)$, where $C_{N, N+J}(y) = [N!/(N+J)!] y^J e^{-y} [L_N^J(y)]^2$ with $L_N^J(y)$ being the associated Laguerre polynomial.

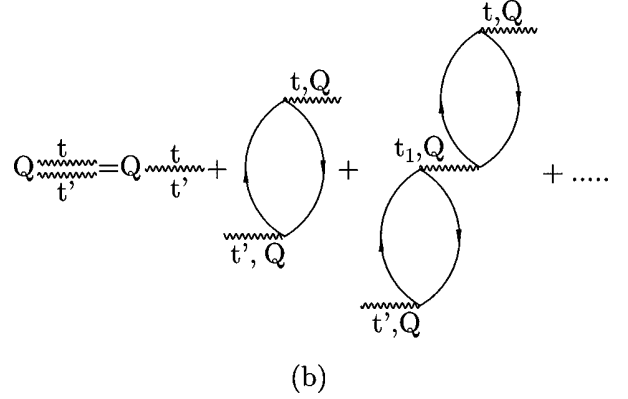
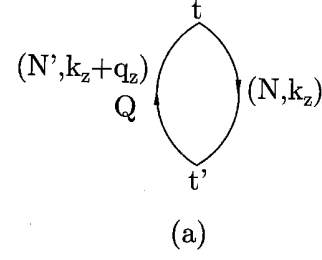


FIG. 1. Diagrams for an electron gas in (\mathbf{Q}, t) representation: (a) the pair bubble or electron density-density correlation function and (b) the effective electron-electron interaction under the random-phase approximation.

Following the standard approach to calculate the pair bubble for a Fermi system at finite temperatures,¹⁵ the electron $d-d$ correlation function in the (\mathbf{Q}, t) representation is obtained as

$$\begin{aligned} \Pi(\mathbf{Q}; t, t') &= \frac{i}{\hbar} \Theta(t-t') e^{-ir_0 q_x [\cos(\omega t) - \cos(\omega t')]} \frac{g_s}{2\pi l^2} \\ &\times \sum_{N', N} C_{N', N}(l^2 q^2/2) \sum_{k_z} \\ &\times \{f[E_N(k_z) + E_{em}] - f[E_{N'}(k_z + q_z) + E_{em}]\} \\ &\times e^{-i[E_N(k_z) - E_{N'}(k_z + q_z)](t-t')/\hbar}, \end{aligned} \quad (3)$$

where $f(x) = [e^{(x-E_F)/k_B T} + 1]^{-1}$ is the Fermi-Dirac function with E_F the Fermi energy.

The Fourier transform (or average over time $t-t'$) of the electron $d-d$ correlation function is given, after generating $e^{ix \cos y}$ into the Bessel functions, by

$$\begin{aligned} \Pi(\mathbf{Q}, \Omega; t') &= \sum_{m, m'=-\infty}^{\infty} i^{m'-m} J_m(r_0 q_x) J_{m'}(r_0 q_z) \\ &\times e^{i(m+m')\omega t'} \Pi_0(\mathbf{Q}, \Omega + m\omega). \end{aligned} \quad (4)$$

Here, an infinitesimal quantity $i\delta$ has been introduced to make the integral converge, $J_m(x)$ is a Bessel function, and

$$\Pi_0(\mathbf{Q}, \Omega) = \frac{g_s}{2\pi l^2} \sum_{N', N} C_{N', N} (l^2 q^2 / 2) \sum_{k_z} \frac{f[E_N(k_z) + E_{em}] - f[E_{N'}(k_z + q_z) + E_{em}]}{\hbar \Omega + E_N(k_z) - E_{N'}(k_z + q_z) + i\delta}. \quad (5)$$

At a steady state, we can average the initial time t' in $\Pi(\mathbf{Q}, \Omega; t')$ over a period of the radiation field.¹⁷ Thus, the Fourier transform of the electron d - d correlation in Ω space (i.e., frequency-space) becomes

$$\Pi(\mathbf{Q}, \Omega) = \sum_{m=-\infty}^{\infty} J_m^2(r_0 q_z) \Pi_0(\mathbf{Q}, \Omega + m\omega). \quad (6)$$

When $F_0 = 0$ so that $r_0 = \gamma = 0$ and $J_m^2(0) = \delta_{0,m}$, $\Pi(\mathbf{Q}, \Omega) = \Pi_0(\mathbf{Q}, \Omega)$ [cf. Eq. (5)] is the well-known result obtained in the absence of the EM field.

IV. RPA DIELECTRIC FUNCTION

The dielectric function measures the response of the electron gas to an applied external charge density. With the electron d - d correlation function given above, we can determine the dynamical dielectric function in the presence of the intense laser radiation. In the present study, I limit myself to the case where the calculation is carried out within the random-phase approximation (RPA). In the (\mathbf{Q}, t) representation, the RPA diagrams for e - e interaction are given by Fig. 1(b) and the effective e - e interaction can be calculated through

$$\begin{aligned} -iV_{\text{eff}}(\mathbf{Q}; t, t') &= [-iV_Q] \delta(t-t') + [-iV_Q] [-i\Pi(\mathbf{Q}; t, t')] \\ &\times [-iV_Q] + \int_{t'}^t dt_1 [-iV_Q] \\ &\times [-i\Pi(\mathbf{Q}; t_1, t')] \\ &\times [-iV_Q] [-i\Pi(\mathbf{Q}; t, t_1)] [-iV_Q] + \dots \end{aligned} \quad (7)$$

Here, $V_Q = 4\pi e^2 / \kappa Q^2$ is the Fourier transform of the bare e - e interaction induced by the Coulomb potential, with κ the dielectric constant of the material. In the (\mathbf{Q}, t) space, the bare e - e interaction in an electronic system is time independent. Introducing Eq. (3), the pair bubble in the (\mathbf{Q}, t) space, into Eq. (7), the effective e - e interaction can be written as

$$V_{\text{eff}}(\mathbf{Q}; t, t') = \frac{V_Q}{\epsilon(\mathbf{Q}; t, t')}. \quad (8)$$

Hence, by definition, the inverse dielectric function of an electron gas in t space is

$$\begin{aligned} \frac{1}{\epsilon(\mathbf{Q}; t, t')} &= \delta(t-t') + \frac{i}{\hbar} \Theta(t-t') e^{-ir_0 q_z [\cos(\omega t) - \cos(\omega t')]} \\ &\times \sum_{j=1}^{\infty} \left[-\frac{g_s}{2\pi l^2} V_Q \right]^j I_j(\mathbf{Q}; t-t'). \end{aligned} \quad (9)$$

Using the following notations

$$C_j = C_{N', N_j} (l^2 q^2 / 2), \quad (10a)$$

$$\Delta f_j = f[E_{N_j}(k_j) + E_{em}] - f[E_{N'_j}(k_j + q_z) + E_{em}], \quad (10b)$$

and

$$\Delta E_j = E_{N'_j}(k_j + q_z) - E_{N_j}(k_j), \quad (10c)$$

the term $I_j(\mathbf{Q}; \tau)$ in Eq. (9) is given by

$$I_1(\mathbf{Q}; \tau) = \sum_{N'_1, N_1} C_1 \sum_{k_1} \Delta f_1 e^{-i\Delta E_1 \tau / \hbar}, \quad (11a)$$

$$\begin{aligned} I_2(\mathbf{Q}; \tau) &= \sum_{N'_1, N_1; N'_2, N_2} C_1 C_2 \sum_{k_1, k_2} \Delta f_1 \Delta f_2 \\ &\times \left[\frac{e^{-i\Delta E_1 \tau / \hbar}}{\Delta E_1 - \Delta E_2} + \frac{e^{-i\Delta E_2 \tau / \hbar}}{\Delta E_2 - \Delta E_1} \right]; \end{aligned} \quad (11b)$$

and

$$\begin{aligned} I_j(\mathbf{Q}; \tau) &= \sum_{N'_1, N_1; N'_2, N_2; \dots; N'_j, N_j} C_1 C_2 \dots C_j \\ &\times \sum_{k_1, k_2, \dots, k_j} \Delta f_1 \Delta f_2 \dots \Delta f_j \\ &\times \left[\frac{e^{-i\Delta E_1 \tau / \hbar}}{[\Delta E_1 - \Delta E_2] \dots [\Delta E_1 - \Delta E_j]} \right. \\ &\left. + \dots + \frac{e^{-i\Delta E_j \tau / \hbar}}{[\Delta E_j - \Delta E_{j-1}] \dots [\Delta E_j - \Delta E_1]} \right]. \end{aligned} \quad (11c)$$

The Fourier transform of the inverse dielectric function is given, after generating $e^{ix \cos y}$ terms in Eq. (9) into the Bessel functions, by

$$\begin{aligned} \frac{1}{\epsilon(\mathbf{Q}, \Omega; t')} &= \sum_{m, m' = -\infty}^{\infty} \\ &\times \frac{i^{m'-m} J_m(r_0 q_z) J_{m'}(r_0 q_z) e^{i(m+m')\omega t'}}{1 - V_Q \Pi_0(\mathbf{Q}, \Omega + m\omega)}. \end{aligned} \quad (12)$$

At a steady state, after averaging t' in $1/\epsilon(\mathbf{Q}, \Omega; t')$ over a period of the radiation field, the Fourier transform of the inverse dielectric function in Ω space is obtained as

$$\frac{1}{\epsilon(\mathbf{Q}, \Omega)} = \sum_{m=-\infty}^{\infty} \frac{J_m^2(r_0 q_z)}{1 - V_Q \Pi_0(\mathbf{Q}, \Omega + m\omega)}. \quad (13)$$

When $F_0 = 0$ so that $r_0 = \gamma = 0$ and $J_m^2(0) = \delta_{0,m}$, $\epsilon(\mathbf{Q}, \Omega) = 1 - V_Q \Pi_0(\mathbf{Q}, \Omega)$ is the well-known result obtained in the absence of the EM field.

V. RESULTS AND DISCUSSIONS

In the presence of an EM radiation, electrons in the system can interact with the radiation field via the processes of photon absorption and emission. The index m in Eqs. (6) and (13) corresponds to the emission ($m < 0$) or absorption ($m > 0$) of m photons, which reflects the fact that the emission and absorption of photons by electrons can be achieved via multiphoton channels where $|m| > 1$. When an electron gas is subjected to an intense EM field, the energy of the electronic system will be blueshifted by that of the radiation field (i.e., by a factor $E_{em} = 2\gamma\hbar\omega$) due to the dynamical Franz-Keldysh effect.¹⁷ This effect can be seen in the electron d - d correlation function [cf. Eqs. (3), (5), and (6)] and in the inverse dielectric function [cf. Eqs. (9) and (13)].

From the results shown above, we see that the response of an electron gas to a time-dependent driving field such as an EM field depends not only on the time difference $t-t'$ but also on the time shift. As a consequence, the Green's function, the d - d correlation function and the inverse dielectric function in the t space are basically the two-time quantities. To study the steady-state behavior of a two-time quantity, one may Fourier analyse it according first to relative coordinate (i.e., $\tau = t-t'$) then to time "center of mass" (i.e., $T = (t+t')/2$).¹⁸ However, for the case of an EM field that is periodic in time, when the time scale of the measurement is much larger than $1/\omega$, one normally does not do Fourier analysis along the T direction instead of averaging t' or t over a period of the radiation field. The latter approach has been employed in the present study. It should be noted that $1/\epsilon(\mathbf{Q}, \Omega)$ [Eq. (13)] determined from $1/\epsilon(\mathbf{Q}; t, t')$ [Eq. (9)] by using this approach (method I) differs sharply to that obtained from directly using the RPA diagrams in Ω space associated with the pair bubble in the (\mathbf{Q}, Ω) representation (method II). In the absence of the EM field, method I and II lead to an identical final result. However, the presence of the time-dependent driving field such an EM radiation implies that method I is the only way to evaluate correctly the inverse dielectric function in the Ω space. Furthermore, it is interesting to point out that in the present study, the usage of generating $e^{ix \cos y}$ into the Bessel functions results in the

complete spectrum of a two-time quantity [e.g., $1/\epsilon(\mathbf{Q}; t, t')$ or $\Pi(\mathbf{Q}; t, t')$] being present in the τ direction and only the zeroth term of it existing in the T direction (here $T = t'$). This result *looks like* the fast approximation.¹⁸ However, in contrast to the normal fast approximation, here we do not introduce any approximation regarding the spectrum in the τ and T direction and there is no limit of the frequency range within which the approach holds. Therefore, in the above obtained theoretical results the effect of the radiation field is included exactly. Moreover, it should be noted that in contrast to Ref. 17 where one paper dealt with the dc case and in another paper the time average was calculated over $T = (t+t')/2$, in the present study I calculate the average over the initial time t' . As can be seen, this approach is more transparent and leads to a much simpler final result.

From now on, I discuss the influence of the linearly polarized EM radiation on static dielectric function (i.e., for the case of $\Omega = 0$) in the low-temperature limit (i.e., $T \rightarrow 0$).

A. Analytical results

In the $T \rightarrow 0$ limit, from Eq. (13) the real and imaginary parts of the inverse dielectric function for $\Omega = 0$ are given, respectively, by

$$\text{Re} \left[\frac{1}{\epsilon(\mathbf{Q}, 0)} \right] = \frac{Q^2 |q_z|}{K_0^3} \sum_{m=-\infty}^{\infty} \frac{J_m^2(r_0 q_z) [Q^2 |q_z| / K_0^3 - R_1(\mathbf{Q}, m\omega)]}{[Q^2 |q_z| / K_0^3 - R_1(\mathbf{Q}, m\omega)]^2 + R_2^2(\mathbf{Q}, m\omega)}, \quad (14a)$$

and

$$\text{Im} \left[\frac{1}{\epsilon(\mathbf{Q}, 0)} \right] = -\frac{Q^2 |q_z|}{K_0^3} \sum_{m=-\infty}^{\infty} \frac{J_m^2(r_0 q_z) R_2(\mathbf{Q}, m\omega)}{[Q^2 |q_z| / K_0^3 - R_1(\mathbf{Q}, m\omega)]^2 + R_2^2(\mathbf{Q}, m\omega)}, \quad (14b)$$

where

$$R_1(\mathbf{Q}, \Omega) = \sum_{N', N} C_{N', N}(l^2 q^2 / 2) \left[\Theta(E_F - E_{em} - E_N) \ln \frac{\hbar\Omega + E_N - E_{N'} - \varepsilon_{q_z} + 2\sqrt{\varepsilon_{q_z}(E_F - E_{em} - E_N)}}{\hbar\Omega + E_N - E_{N'} - \varepsilon_{q_z} - 2\sqrt{\varepsilon_{q_z}(E_F - E_{em} - E_N)}} \right. \\ \left. - \Theta(E_F - E_{em} - E_{N'}) \ln \frac{\hbar\Omega + E_N - E_{N'} + \varepsilon_{q_z} + 2\sqrt{\varepsilon_{q_z}(E_F - E_{em} - E_{N'})}}{\hbar\Omega + E_N - E_{N'} + \varepsilon_{q_z} - 2\sqrt{\varepsilon_{q_z}(E_F - E_{em} - E_{N'})}} \right], \quad (14c)$$

and

$$R_2(\mathbf{Q}, \Omega) = \pi \sum_{N', N} C_{N', N}(l^2 q^2 / 2) \{ \Theta[4\varepsilon_{q_z}(E_F - E_{em} - E_N) - (\hbar\Omega + E_N - E_{N'} - \varepsilon_{q_z})^2] - \Theta[4\varepsilon_{q_z}(E_F - E_{em} - E_{N'}) - (\hbar\Omega + E_N - E_{N'} + \varepsilon_{q_z})^2] \}. \quad (14d)$$

Here, $\varepsilon_{q_z} = \hbar^2 q_z^2 / 2m^*$ and $K_0^3 = 2e^2 m^* / (\pi \hbar^2 l^2 \kappa)$. From Eq. (14) we see that in the presence of the EM and magnetic fields, the dielectric function of an electron gas results from electronic transitions via: (i) intra- and inter-LL channels; (ii) different optical processes including multiphoton channels; and (iii) the variation of electron wave vector (or momentum) along different directions.

For the case of $q_z \rightarrow 0$, because $\lim_{x \rightarrow 0} J_m^2(x) = \delta_{m,0}$, we have

$$\text{Re} \left[\frac{1}{\epsilon(q,0)} \right] = \frac{q^2}{q^2 - 2K_0^3 \sum_{N',N} C_{N',N}(l^2 q^2/2) R_{N',N}}, \quad (15a)$$

and

$$\text{Im} \left[\frac{1}{\epsilon(q,0)} \right] = 0, \quad (15b)$$

where $R_{N',N} = [\Theta(E_F - E_{em} - E_N) K_{F,N}^* - \Theta(E_F - E_{em} - E_{N'}) K_{F,N'}^*] l^2 / (N - N')$ for $N \neq N'$ and $R_{NN} = \Theta(E_F - E_{em} - E_N) / K_{F,N}^*$, with $K_{F,N}^* = [2m^*(E_F - E_{em} - E_N) / \hbar^2]^{1/2}$. Equation (15) indicates that for dielectric response induced by electronic transition events in which the electron wave vector k_z is not varied, (1) the imaginary part of the static dielectric function is zero; (2) the electronic transitions are not accompanied by emission and absorption of photons; (3) the influence of the EM radiation on dielectric function is achieved mainly via varying the Fermi energy of the system (see Ref. 14) and the energy of the radiation field; and (4) the dielectric response results mainly from intra- and inter-LL transitions with only the change \mathbf{q} of electron wave vector in the xy plane. Therefore, the case of $q_z = 0$ is an ideal configuration to study dielectric response induced by electronic transitions via intra- and inter-LL channels.

For the case of $q \rightarrow 0$, because $\lim_{x \rightarrow 0} C_{N',N}(x) = \delta_{N',N}$, the real and imaginary parts of the inverse static dielectric function are given, respectively, by

$$\text{Re} \left[\frac{1}{\epsilon(q_z,0)} \right] = \frac{|q_z|^3}{K_0^3} \sum_{m=-\infty}^{\infty} \frac{J_m^2(r_0 q_z) [|q_z|^3 / K_0^3 - R_m(q_z)]}{[|q_z|^3 / K_0^3 - R_m(q_z)]^2 + I_m^2(q_z)}, \quad (16a)$$

and

$$\text{Im} \left[\frac{1}{\epsilon(q_z,0)} \right] = - \frac{|q_z|^3}{K_0^3} \sum_{m=-\infty}^{\infty} \frac{J_m^2(r_0 q_z) I_m(q_z)}{[|q_z|^3 / K_0^3 - R_m(q_z)]^2 + I_m^2(q_z)} = 0, \quad (16b)$$

where

$$R_m(q_z) = \sum_N \Theta(E_F - E_{em} - E_N) \times \ln \frac{(m\hbar\omega)^2 - \epsilon_{q_z} (\sqrt{\epsilon_{q_z}} - 2\sqrt{E_F - E_{em} - E_N})^2}{(m\hbar\omega)^2 - \epsilon_{q_z} (\sqrt{\epsilon_{q_z}} + 2\sqrt{E_F - E_{em} - E_N})^2}, \quad (16c)$$

and

$$I_m(q_z) = \pi \sum_N \{ \Theta[4\epsilon_{q_z}(E_F - E_{em} - E_N) - (m\hbar\omega - \epsilon_{q_z})^2] - \Theta[4\epsilon_{q_z}(E_F - E_{em} - E_N) - (m\hbar\omega + \epsilon_{q_z})^2] \}. \quad (16d)$$

Equation (16) shows that for the dielectric response caused by electronic transitions in which the electron wave vector along the xy plane keeps constant, (1) the contribution from different optical processes to $\text{Im}[\epsilon(q_z,0)]^{-1}$ can be observed;

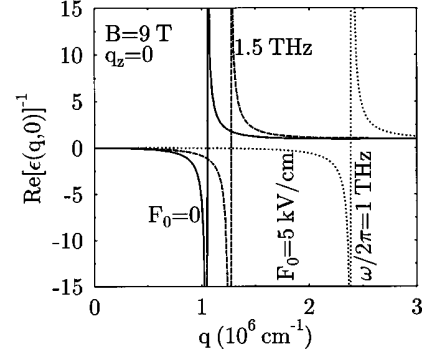


FIG. 2. Real part of the inverse static dielectric function at $q_z = 0$ as a function of electron wave vector q in the xy plane at a fixed magnetic field B for different EM radiation fields: (i) the absence of the radiation (solid curve); (ii) $F_0 = 5$ kV/cm and $f = \omega/2\pi = 1$ THz (dotted curve) and (iii) $F_0 = 5$ kV/cm and $f = 1.5$ THz (dashed curve).

(2) however, when both optical emission and absorption are possible, the overall contribution of the optical processes to $\text{Im}[\epsilon(q_z,0)]^{-1}$ is vanished, because $I_{-m}(q_z) = -I_m(q_z)$ [see Eq. (16d)]; (3) the dielectric response occurs through intra-LL transitions with only the change q_z of electron wave vector along the z direction; (4) the contribution to $\text{Re}[\epsilon(q_z,0)]^{-1}$ from optical emission is the same as that from optical absorption, because $R_{-m}(q_z) = R_m(q_z)$ [see Eq. (16c)]; and (5) the dielectric response can be accompanied by the events of photon emission and absorption. Hence, the case of $q = 0$ can be used to study the dielectric response caused by electronic transitions via different optical processes.

B. Numerical results

The numerical results of this paper pertain to GaAs-based 3DEG structures. For GaAs, the effective electron mass is $m^* = 0.0665m_e$, with m_e being the rest electron mass and the dielectric constant is $\kappa = 12.9$. Further, I consider a n -type-doped GaAs with the typical electron density $N_e = 10^{17} \text{ cm}^{-3}$. The calculation of the Fermi energy in the presence of EM and magnetic fields has been documented in Ref. 14. In the results shown below, the contributions from $m = 0, \pm 1, \pm 2, \dots$ and ± 20 are included. The inclusion of more m affects only the results in low-frequency radiations.

The real part of inverse dielectric function for the case of $q_z = 0$ is plotted in Fig. 2 as a function of electron wave vector q in the xy plane for different radiation fields. When $q_z = 0$, the dielectric response via emission and absorption of photons by electrons is impossible and, therefore, $\text{Re}[\epsilon(q,0)]^{-1}$ has the usual features: (1) for small (large) values of q , $\text{Re}[\epsilon(q,0)]^{-1}$ is negative (positive) and decreases with increasing q and (2) with varying q so that $q^2 \sim 2K_0^3 \sum_{N',N} C_{N',N}(l^2 q^2/2) R_{N',N}$, the singularity can be observed. The feature (2) is electrically analogous to the Kohn effect¹ observed in a 3DEG in the absence of the radiation and magnetic fields when $q \sim 2K_F$. It should be noted that in the presence of the EM radiation, the Fermi energy depends on frequency ω and intensity F_0 of the radiation field.¹⁴ Thus, the conditions under which the Kohn effect is measurable can be varied through varying F_0 and/or ω .

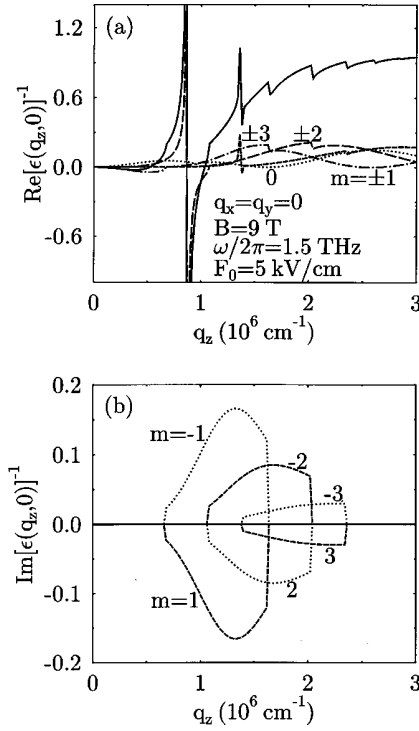


FIG. 3. Contribution from different optical processes to real [in (a)] and imaginary [in (b)] parts of the inverse static dielectric function for $q=0$ at a fixed magnetic field and a fixed radiation field. $m>0$ and $m<0$ correspond, respectively, to the process of m -photon absorption and emission. The solid curve is the total inverse dielectric function.

The contribution from different optical processes to real and imaginary parts of the inverse dielectric function for the case of $q=0$ is shown in Fig. 3 at the fixed radiation and magnetic fields. $q_z \neq 0$ makes it possible to achieve dielectric response via electronic transitions accompanied by emission and absorption of photons by electrons (see Fig. 3). For the case of $q=0$, the inter-LL transitions do not contribute to the dielectric function, and the 0-photon process does not affect the imaginary part of the static dielectric function. For small values of q_z , photon emission and absorption have no effect on $\text{Im}[\epsilon(q_z, 0)]^{-1}$. With increasing q_z , the contributions from different optical processes to imaginary part of the dielectric function can be observed [see Fig. 3(b)], although the overall contributions due to the optical emission and absorption is zero at $q=0$. We note that the singular feature of $\text{Re}[\epsilon(q_z, 0)]^{-1}$ (i.e., the Kohn effect) can only be observed when $I_m(q_z) = 0$ [see Eq. (16)], which happens only for small values of q_z [see Fig. 3(b)]. Within the regime where $I_m(q_z) = 0$, the singularity of $\text{Re}[\epsilon(q_z, 0)]^{-1}$ at a fixed Fermi energy E_F is induced only by some particular optical processes when the condition $|q_z|^3 \sim K_0^3 R_m(q_z)$ is satisfied. For example, the Kohn effect observed in Fig. 3(a) is associated with the two-photon emission and absorption processes, and other optical processes do not cause the Kohn effect although some step changes induced by these processes can be observed. By changing E_F via varying, e.g., F_0 and/or ω , we can observe the Kohn effect induced by different photon processes. Hence, in the presence of the intense EM radiation, one can study the influence of different optical processes on

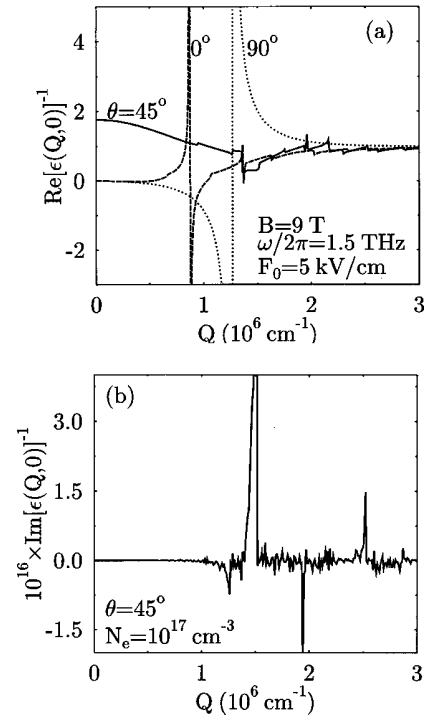


FIG. 4. Real [in (a)] and imaginary [in (b)] parts of the inverse static dielectric function as a function of electron wave vector \mathbf{Q} at a fixed radiation field and a fixed magnetic field for different θ angles. Here, θ is the polar angle. Note that when $\theta=0$ or 90° , $\text{Im}[\epsilon(\mathbf{Q}, 0)]^{-1} = 0$.

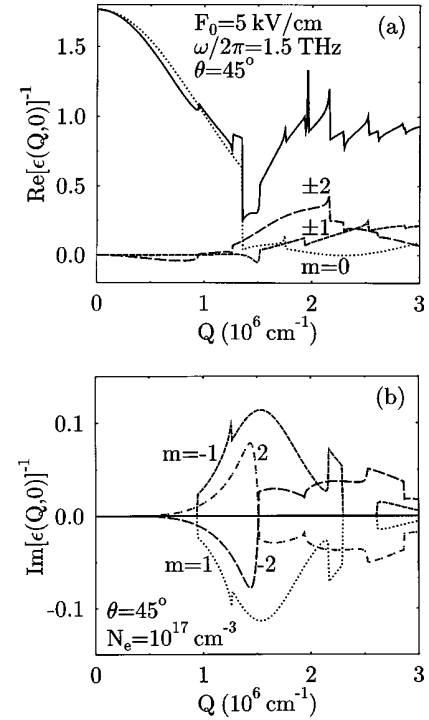


FIG. 5. Contribution from different optical processes to real [in (a)] and imaginary [in (b)] parts of the inverse static dielectric function for $\theta=45^\circ$ at a fixed magnetic field and a fixed radiation field.

dielectric response of an electron gas, through measuring the Kohn effect by varying ω and/or F_0 of the radiation field.

Figure 4 shows the results for real and imaginary parts of the inverse dielectric function obtained in different geometries, i.e., for different angles of θ . Here we define $q_z = Q \cos \theta$ and $q = Q \sin \theta$ with θ being the polar angle. From Eq. (14), we see that in general, the singularity of $\text{Re}[\epsilon(\mathbf{Q},0)]^{-1}$ can be observed: (i) when $R_2(\mathbf{Q},m\omega)=0$, which occurs for small values of Q , see Fig. 5(b), and (ii) when the condition $Q^2|q_z| \sim K_0^3 R_1(\mathbf{Q},m\omega)$ is satisfied. The results shown in Fig. 4(a) indicate that at the fixed radiation and magnetic fields where the Kohn effect may be observed for $\theta=0$ (i.e., $q=0$) and for $\theta=90^\circ$ (i.e., $q_z=0$), the singular nature of $\text{Re}[\epsilon(\mathbf{Q},0)]^{-1}$ may not be seen for $\theta=45^\circ$, where the conditions (i) and (ii) are not satisfied simultaneously. Moreover, it is well known that in the absence of the EM radiation field, $\text{Im}[\epsilon(\mathbf{Q},0)]^{-1}$ is always zero. In contrast, the presence of the intense EM radiation will result in a nonzero $\text{Im}[\epsilon(\mathbf{Q},0)]^{-1}$, when $\theta \neq 0$ or $\theta \neq 90^\circ$ [see Fig. 4(b)], although this effect is very weak. When $q \neq 0$ and $q_z \neq 0$, the dielectric response of an electron gas can be achieved by the intra- and inter-LL transitions around the Fermi level, accompanied by the emission and absorption of photons. From the fact that the imaginary part of the inverse dielectric function measures the electron-energy loss (or gain) via photon emission (or absorption), the presence of the channels for inter-LL transitions may lead to the consequence that the energy that an electron gains from the radiation field via photon absorption may not be compensated by that which an electron loses via photon emission. As a result, a nonzero $\text{Im}[\epsilon(\mathbf{Q},0)]^{-1}$ can be observed.

The contribution from different optical processes to real and imaginary parts of the inverse dielectric function measured at $\theta=45^\circ$ is shown in Fig. 5 at the fixed radiation field and fixed magnetic field. Compared with those shown in Fig. 3 for $\theta=0$, we see that the effect of different optical processes on dielectric function may differ sharply for different θ angles. The physical reason behind this is that the variation of θ results in the variation of the possibility for electronic transitions via different optical and LL channels with the change Q of the electron wave vector. Therefore, the dielectric function of an electron gas subjected to intense EM radiation and to quantizing magnetic field is highly anisotropic.

VI. CONCLUSIONS

In this paper, I have derived the electron density-density correlation function and the RPA dielectric function for an ideal 3DEG subjected to linearly polarized EM field and to static quantizing magnetic field. The dependence of the inverse dielectric function on frequency and intensity of the EM radiation and on different optical processes has been examined theoretically. The main results obtained from this study are summarized as follows.

Using theoretical approaches developed in this paper, the effect of electron interactions with the radiation field can be included exactly in the evaluation of the quantities such as the electron d - d correlation function and dielectric function in t and Ω space. When an electron gas is subjected to linearly polarized THz laser field and to strong static magnetic field, the electron d - d correlation function and the effective

electron-electron interaction will be modified strongly by frequency and intensity of the radiation field. Both optical emission and absorption contribute to the d - d correlation function and to the RPA dielectric function. In this case, the RPA dielectric function of an electron gas results from: (i) intra- and inter-LL electronic transitions; (ii) different optical processes including multiphoton emission and absorption; and (iii) the variation \mathbf{Q} of electron wave vector (or momentum). By looking into the dependence of the inverse dielectric function on \mathbf{Q} along different directions, we can study the dielectric response caused by different optical processes and by different LL transition events. For example, the case of $q_z=0$ ($q=0$) can be used to study the dielectric response induced by electronic transitions via intra- and inter-LL channels (via different processes of photon emission and absorption).

When a 3DEG is subjected to intense THz EM radiation in strong magnetic fields, the singular feature of the real part of the inverse dielectric function, i.e., the Kohn effect, can be observed for relatively small values of Q . The presence of the EM field will lead to more strict conditions to observe the Kohn effect, in comparison with the situation where the radiation is absent. For an electronic system with a fixed Fermi level, the Kohn effect observed in the presence of the intense THz radiation is connected to some particular optical processes associated with the emission and absorption of photons. By changing the Fermi energy through varying, e.g., intensity and/or frequency of the radiation field, we can study the influence of different optical processes on dielectric response of an electron gas, through measuring the Kohn effect.

Under the intense EM radiations, the imaginary part of the static dielectric function of a 3DEG in strong magnetic fields may be nonzero for the case of $q_z \neq 0$ and $q \neq 0$. This effect is a consequence of inter-LL electronic transitions around the Fermi level, accompanied by emission and absorption of photons by electrons. Moreover, by varying \mathbf{Q} the electron wavevector along the different directions, one can vary the possibility for electronic transitions via different optical processes and via different LL channels and, consequently, one can study the dielectric response induced by different electronic transition mechanisms.

When a GaAs-based 3DEG is subjected to an intense THz EM field and to a quantizing magnetic field, the electron-kinetic energy and the Fermi and cyclotron energies are comparable to THz photon energy $\hbar\omega$ and to that of the radiation field $E_{em}=2\gamma\hbar\omega$. As a consequence, the THz EM field can couple strongly to the electron-gas system. The influence of an EM radiation on dielectric response of an electron gas is achieved mainly through two parameters: $r_0=eF_0/m^*\omega^2$ and $\gamma=(eF_0)^2/8m^*\hbar\omega^3$. For a GaAs-based 3DEG driven by a linearly polarized laser field with $F_0 \sim 1$ kV/cm and $\omega \sim 1$ THz, which can be realized in present THz FEL sources, the conditions $r_0q_z \sim 1$ and $\gamma \sim 1$ can be satisfied. Hence, the features distinctive for electron-photon interactions can be observed by measuring, e.g., the Fermi energy and the dielectric function using the THz free-electron laser radiation.

ACKNOWLEDGMENT

This work was supported by the Australian Research Council.

*Electronic address: wxu@wumpus.its.uow.edu.au

- ¹For a review on a 3DEG at zero magnetic field, see, e.g., J. M. Ziman, *Principles of the Theory of Solids* (Cambridge University Press, London, 1965).
- ²For a review on a 3DEG in high-magnetic fields, see, e.g., N. J. M. Horing and M. Yildiz, *Ann. Phys. (N.Y.)* **97**, 216 (1976); N. D. Mermin and E. Canel, *ibid.* **26**, 247 (1964).
- ³For a review on a 2DEG at zero magnetic field, see, e.g., T. Ando, A. B. Fowler, and F. Stern, *Rev. Mod. Phys.* **54**, 437 (1982).
- ⁴For a review on a 2DEG in high-magnetic fields, see, e.g., A. Isihara, *Solid State Phys.* **42**, 271 (1989).
- ⁵N. G. Asmar, A. G. Markelz, E. G. Gwinn, J. Černe, M. S. Sherwin, K. L. Campman, P. E. Hopkins, and A. C. Gossard, *Phys. Rev. B* **51**, 18 041 (1995); W. Xu and C. Zhang, *Appl. Phys. Lett.* **68**, 3305 (1996).
- ⁶N. G. Asmar, J. Černe, A. G. Markelz, E. G. Gwinn, M. S. Sherwin, K. L. Campman, and A. C. Gossard, *Appl. Phys. Lett.* **68**, 829 (1996); W. Xu and C. Zhang, *Phys. Rev. B* **55**, 5259 (1997).
- ⁷A. G. Markelz, N. G. Asmar, B. Brar, and E. G. Gwinn, *Appl. Phys. Lett.* **69**, 3975 (1996); W. Xu, *Europhys. Lett.* **40**, 411 (1997).
- ⁸B. N. Murdin, W. Heiss, C. J. G. M. Langerak, S.-C. Lee, I. Galbraith, G. Strasser, E. Gornik, M. Helm, and C. R. Pidgeon, *Phys. Rev. B* **55**, 5171 (1997).
- ⁹C. J. G. M. Langerak, B. N. Murdin, B. E. Cole, J. M. Chamberlain, M. Henini, M. Pate, and G. Hill, *Appl. Phys. Lett.* **67**, 3453 (1995).
- ¹⁰T. A. Vaughan, R. J. Nicholas, C. J. G. M. Langerak, B. N. Murdin, C. R. Pidgeon, N. J. Mason, and P. J. Walker, *Phys. Rev. B* **53**, 16 481 (1996).
- ¹¹P. M. Koenraad, R. A. Lewis, L. R. C. Waumans, C. J. G. M. Langerak, W. Xu, and J. H. Wolter, *Physica B* **256-258**, 268 (1998).
- ¹²W. Xu, *Phys. Status Solidi B* **205**, 559 (1998).
- ¹³W. Xu, *Semicond. Sci. Technol.* **12**, 1559 (1997).
- ¹⁴W. Xu, *J. Phys.: Condens. Matter* **9**, L591 (1997).
- ¹⁵See, e.g., R. D. Mattuck, *A Guide to Feynman Diagrams in the Many-Body Problem* (McGraw-Hill, New York, 1976).
- ¹⁶See, e.g., C. S. Ting, S. C. Ying, and J. J. Quinn, *Phys. Rev. B* **16**, 5394 (1977).
- ¹⁷A. P. Jauho and K. Johnsen, *Phys. Rev. Lett.* **76**, 4576 (1996); R. Bertoni and A. P. Jauho, *Phys. Rev. B* **44**, 3655 (1991).
- ¹⁸See, e.g., T. Brandes, *Phys. Rev. B* **56**, 1213 (1997), and references therein.